Indian Journal of Science and Technology, *Vol 9(44), DOI: 10.17485/ijst/2016/v9i44/101925, November 2016*
ISSN (Print) : 0974-6846
ISSN (Online) : 0974-5645

Application of FPGA Controller in Multidevice Interleaved DC/DC Boost Converter for Air Craft Electrical Systems

D. R. Karthik[1*], B. Mallikarjuna Reddy[2], Kushwaha Satendra Kr Singh[2] and Ahmed Akbar[2]

[1]Department of Electrical Engineering BITS, Hyderabad-501505, Telangana, India; Karthik.dasarathi@gmail.com
[2]Department of Electrical Engineering, MNNIT, Allahabad-211004, UP, India; ree1505@mnnit.ac.in, ree1506@mnnit.ac.in, akbar_ree0713@mnnit.ac.in

Abstract

Background/Objectives: In this paper we study Two pole–Two phase and Four pole-Three phase Multidevice interleaved DC/DC boost converter with FPGA controller to achieve high performance for Aircraft Electrical systems where there is need of high efficiency, high thermal capability with power density. **Methods/Statistical Analysis:** Interleaved DC/DC boost converter has been usage in the power electronics circuits due to its inherent quality of huge reduction in source current ripple and output ripple voltage due to the interleaving of the input supply and multi devices. **Findings:** Multidevice Interleaved DC/DC boost converter has found huge applications due to its advantages like reduced size due to reduction in contribution current and output voltage ripple thereby reducing size of filter machineries. In addition to above advantages low EMI and low electric hassle in switching can be achieved. **Application/Improvements:** In this study employ Electric Motor to power the Aircraft and Batteries to supply power during Night flights connect via Bi-directional DC/DC converter.

Keywords: Aircraft Electrical System, Energy Storage Systems, Field Programmable Gate Array, Multidevice Interleaved DC/DC Boost Converter and PV Cell

1. Introduction

There is a great need for the increase of flight performance in terms of manoeuvrability and thrust with high power density and compact power structure especially in case of solar powered aircrafts where the space and weight of aircraft is of concern, the solar powered aircrafts are light weight, low speed aircrafts which are still in development stage, these aircrafts are powered by electric motors where supplied through solar cells, and through energy storage systems like powerful batteries such as lithium ion batteries during night flights[1,2]. At present these aircraft such as Solar Impulse 2 has maximum speed of 140 km/h with entire aircraft weighting around 2.4 Tons, which can airborne up to 117 hours the important thing need to take into consideration for Electrical or electronics equipment in aircraft systems are its size, power density and thermal capability for the continuous operation during such long flights, interleaved DC/DC converters proved its capability to handle high power densities With lesser size compared to conventional DC/DC converter and interleaved DC/DC converter are very suitable in aircraft applications[3,4].

**Author for correspondence*

Generally in a solar aircraft systems power from PV cells is fed to the motor and is charged to the batteries connected[5,6]. A solar powered aircraft in conjunction with energy storage system such as high power batteries provides feasible solution for night flights[7]. The bidirectional DC/DC converter allows the recharging and recharging of batteries in order to exchange power from solar panel to batteries and between batteries and electric motor during low power or night flights. The proposed model has been shown in Figure 1.

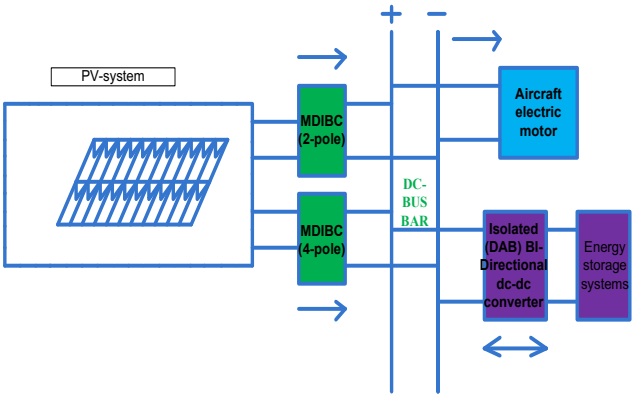

Figure 1. Block diagram of the proposal system.

2. Analysis

A. Photovoltaic Array: A solar cell is an electric scheme which converts photon energy into electricity by the photovoltaic irradiance influence, the solar cell characteristics like current, voltage or resistance vary when exposed to sunshine. Several solar cells in an integrated group called photovoltaic panel or photo voltaic module. The semiconductor wafers are protected from sunlight by covering photovoltaic module with a sheet of glass. As each solar cell has a low voltage level these solar compartments are connected in series to obtain anticipated high voltage and can be connected in parallel to achieve high currents however string of chain cell handled independently, individual power packets often supplied by each module and are connected in parallel these segments can be interconnected to create an array with desired DC voltage and loading current capacity[8].

The Figure 2 shows the ideal photovoltaic cell, the general equation that mathematically demonstrates ideal photovoltaic cell I-V characteristics analysis.

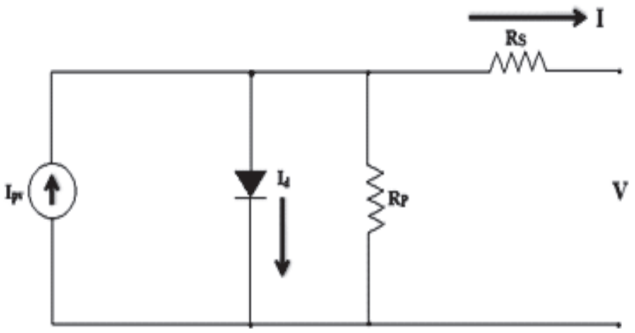

Figure 2 Ideal photovoltaic cell.

$$I = I_p - I_o[e^{(\frac{qv}{\beta kt})} \quad (1)$$

I_p = The photon current generated by the light (in amperes).
I_o = The leakage current of the diode (in amperes).
Q (Electron charge) = 1.602×10^{-19} (in Coulombs).
K (Boltzmann's persistent) = 1.380×10^{-23} (in Joules/Kelvin)
T = Thermal temperature of the p-n junction (in Kelvin).
β = Diode non-ideality factor

However the above equation does not represent I-V characteristics of practical photovoltaic array. The I-V characteristic has been shown in Figure 3.

The current produced by the photovoltaic cell adamantly depends on the solar insolation and is also influenced by the temperature (K) according to the following equation.

$$I_p = (I_p + K_I(T - T_n))\frac{G}{G_n} \quad (2)$$

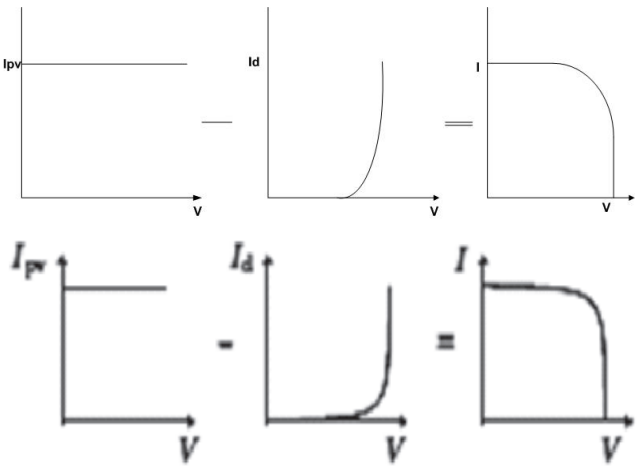

Figure 3. I-V Characteristics of a photovoltaic cell.

I_p =The Photo-generated current at the Reference condition (usually 250°C)

ΔT = T-T_n (T and T_n are the real and standard reference temperatures (in Kelvin)

G = the insolation on the PV surface (in W/m^2)

G_n G_n = Standard reference insolation (in W/m^2)

The diode limitation current I_O and its dependence on the temperature maybe described by

$$I_O = I_o\left(\frac{T_n}{T}\right)e^{\left[\frac{qE_g}{ak}\left(\frac{1}{T_n}-\frac{1}{T}\right)\right]} \quad (3)$$

E_g = The Forbidden Gap energy of the semiconductor n = standard reference saturation current

B. Boost Converters: DC/DC converters are very suitable in renewable applications to boost the low level voltage to a desired voltage level; there are numerous topologies of DC/DC conversion which suits for particular applications. We now discuss basic topologies of boost converter, the basic converters topologies are,

- Simple DC/DC Boost converter
- Multi-device DC/DC Boost converter
- Interleaved DC/DC Boost converter

Simple DC/DC Boost Converter: A Boost converter shown in figure 4 is a generic DC/DC converter where the output voltage is greater than source voltage, to realize a boost converter we should have energy storage device such as inductor and capacitor, a diode and a switch, generally capacitor is placed at output side to filter out ripples in output voltage, and inductor is places at input to reduce ripples in source current[9].

The relation among source voltage (V_s) and output voltage (V_O) is resultant by the volt- second (V-S) balance in the output inductor of the bi-directional DC/DC converter. Because, the voltage wave is periodic and symmetrical wave in the inductor as well as voltage across inductor has been zero over a cycle. It is duty ratio D.

$$\begin{aligned} V_s \times T_{On} &= (V_s - V_O)T_{OFF} \\ V_g \times T_S &= V_O \times T_{Off} \\ \frac{V_O}{V_g} &= \frac{T_S}{T_{Off}} = \frac{1}{(1-D)} \end{aligned} \quad (4)$$

Consider power balance in the whole circuit, current ratio is exactly opposite to the voltage ratio. Due to inductor voltage (V_L), there is a ripple current (ΔI_L) in the output side, ripple current will be derived by the sub cycle of inductor voltage and then integrate the voltage waveform and then get the ripple in the current.

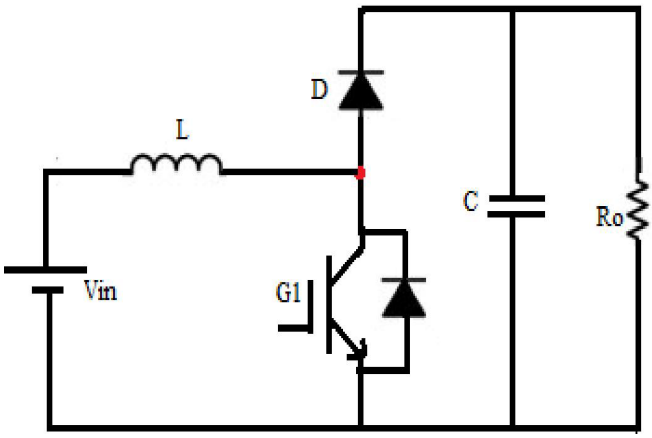

Figure 4. Boost converter.

$$\begin{aligned} &(V_s - I_L R_L)T_{ON} + (V_s - I_L R_L - V_O)T_{Off} \\ &V_s = V_O(1-D) + I_L R_L \\ &V_s = V_O(1-D) + \frac{V_O}{(1-D)}\frac{R_L}{R} \\ &\alpha = \frac{R_L}{R} \\ &\frac{V_O}{V_s} = \frac{1}{(1-D)}\frac{1}{1+\frac{\alpha}{(1-D)^2}} \\ &\frac{V_O}{V_s} = \frac{(1-D)}{(1-D)^2+\alpha} \\ &\frac{I_s}{I_O} = \frac{(1-D)}{1} \\ &\eta = \frac{V_O}{V_s}\times\frac{I_s}{I_O} = \frac{(1-D)^2}{(1-D)^2+\alpha} \end{aligned} \quad (5)$$

Multidevice DC/DC Boost Converter: A Multidevice DC/DC boost converter shown in Figure 5. This type converter has two or more switches linked in parallel to a single inductor; working code is same as that of a boost converter, form m-parallel buttons the dimension of the passive components is reduced by m-times as compared to that of basic boost converter.

Interleaved DC/DC Boost Converter: Interleaved DC/DC boost converter shown in Figure 6 consists of numerous power stages in parallel and compelled with drive signals phase shifted by 360° /k, where k is number of phases, switching frequency (f_s) is increased proportionate to phases. Figure beneath shows two phase inter-leaved boost converter[10].

Each switching device is switched at same frequency but phase shifted by 180° for the two phases. The current is divided into two paths the passage losses can be reduced and eventually increasing overall efficiency[11]. Since two phases are joint at output capacitor effective ripple frequency is doubled, making ripple voltage and ripple current reduction much easier.

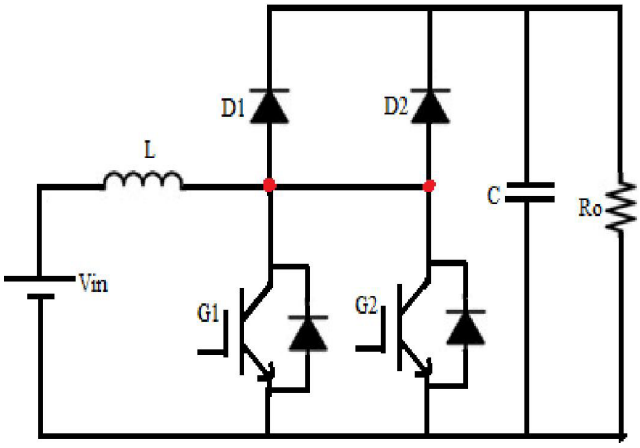

Figure 5. Multi-device boost converter.

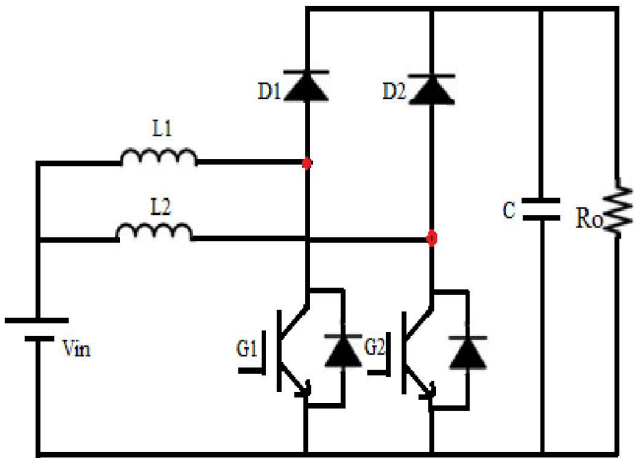

Figure 6. Inter-leaved Boost converter.

3. State Space Analysis of MDIBC

State space describes a mathematical tactic for analysis of the DC/DC converter as a continuous linear system (CLS). By the state space approach, determine the output voltage and currents, the obtained equivalent circuit offers for the physical prototypical of the switching converter, moreover assume ideal elements for this scrutiny and chose inductor current and capacitor voltage as state variables.

A. On State Mode: The on state configuration of MDIBC is shown in Figure 7.

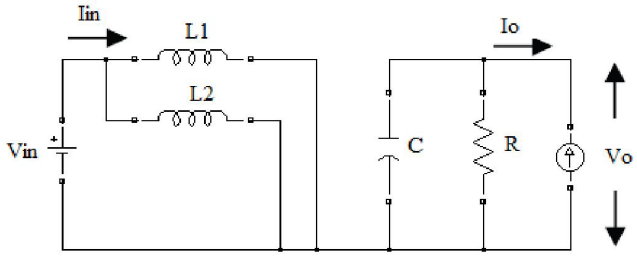

Figure 7. On state operation of MDIBC.

$$L = \frac{L_1 \times L_2}{L_1 + L_2} \tag{6}$$

$$V_{in} = L \times \frac{di_{in}}{dt} \tag{7}$$

$$I_o = C \times \frac{dv_o}{dt} + \frac{V_o}{R} \tag{8}$$

$$\frac{d}{dt}\begin{pmatrix} I_{in} \\ V_o \end{pmatrix} = \begin{pmatrix} 0 & 0 \\ 0 & -\frac{1}{rc} \end{pmatrix}\begin{pmatrix} I_{in} \\ V_o \end{pmatrix} + \begin{pmatrix} \frac{1}{L} & 0 \\ 0 & \frac{1}{c} \end{pmatrix}\begin{pmatrix} V_{in} \\ I_o \end{pmatrix} \tag{9}$$

B. Off State Mode: The off state configure of MDIBC is shown in Figure 8.

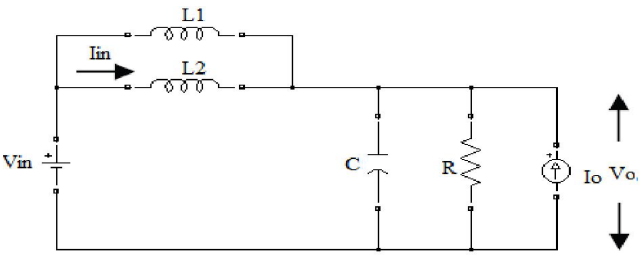

Figure 8. Off state operation of MDIBC.

$$\frac{d}{dt}\begin{pmatrix} I_{in} \\ V_o \end{pmatrix} = \begin{pmatrix} 0 & -\frac{1}{L} \\ \frac{1}{c} & -\frac{1}{rc} \end{pmatrix}\begin{pmatrix} I_{in} \\ V_o \end{pmatrix} + \begin{pmatrix} \frac{1}{L} & 0 \\ 0 & \frac{1}{c} \end{pmatrix}\begin{pmatrix} V_{in} \\ I_o \end{pmatrix} \tag{10}$$

State space averaging,

$$\dot{X} = Ax + Bu \tag{11}$$

4. Proposed Structure of MDIBC

The structure of the proposed converter is shown in Figure 9 and the digital control structure is shown in Figure 10. The converter of two-phase interleaved DC/DC converter consists of two switches and two diodes connected in parallel per phase and figure 11 is a converter of three phases, four switches and four diodes connected in parallel per phase as discussed in preceding section interleaving technique where gate signals are supplied with the phase shift but same frequency. The FPGA Control structure of Four-pole Three-phase structure is shown in Figure 12.

The proposed converter the switching pattern is shifted by 360o/(k × *l*), where k is no of channels or phases &*l* is number of parallel power switches per phase, i.e., poles in our case by employing this interleaving technique the input current and output voltage ripple is the two converters one with two pole two- two phase and four pole-three phase structures have been studied and their presentation characteristics are compared interleaving technique provides to operate four times frequency for two-pole two-phase structure and 12 times four-pole three-phase structure in inductor current at the same switching frequency.

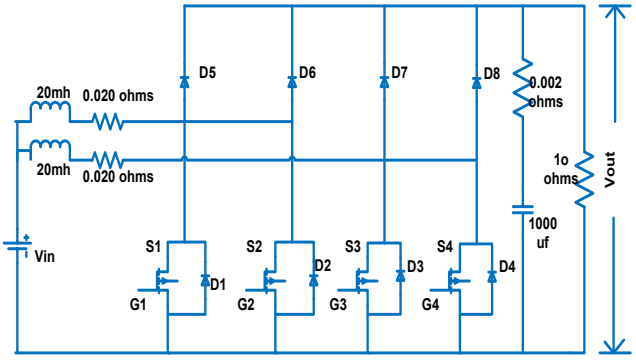

Figure 9. Structure of two-pole two-phase MDIBC.

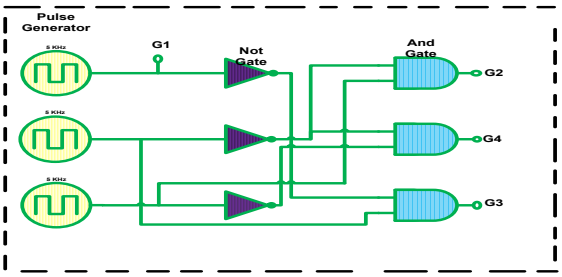

Figure 10. FPGA Control structure for two-pole two-phase MDIBC.

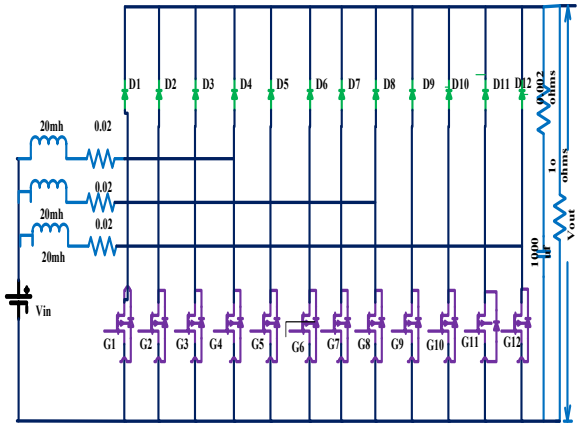

Figure 11. Structure of Two-pole Three-phase MDIBC.

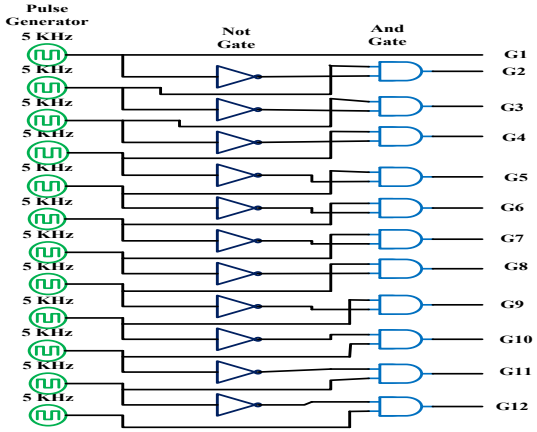

Figure 12. FPGA Control structure of Four-pole Three-phase structure.

As a result the size of inactive components is reduced by k-times associated with the *n*-phase interleaved DC/DC converter.

The output voltage is,

$$V_o = \frac{V_{in}}{(1 - mD)} \tag{12}$$

The input inductor value of MDIBC of (4-pole, 3-phase) is

$$L = \frac{V_S \times D}{m \times n \times f_s \times \Delta I_L} \tag{13}$$

The output capacitor value of MDIBC of (4-pole, 3-phase) is given by

$$C = \frac{I_o \times D}{m \times n \times f_s \times \Delta V} \tag{14}$$

The gate pulses to turn on switches are controlled by field programmable gate array technique (FPGA) this

technique uses logic gates to implement complex digital reckonings, FPGA has capability of reprogramming depending on the need and has dynamic response with high performance which suits best for the proposed converter in it application of aircraft systems.

5. PSCAD Simulation Results

In this segment the Multi-device inter-leaved boost converter are planned and comprehended Two-pole two-phase and Four-pole three-phase using PSCAD software and obtained results are compared. These results are obtained for resistive load of 10 Ohm with gate switching frequency of 5 KHz with input voltage of 200 volts.

Two-Pole Two-Phase (MDIBC): For two-pole two phase structure[12] the output voltage obtained is around 400 Volts and the output current is around 40 Ampere which is shown in Figure 13 and 14 respectively. The wrinkle content is reduced when compared to boost converter, which in turn reduces the size of the filters.

Four-Pole Three-Phase (MDIBC): Output voltage and output current waveforms of a Three-phase four pole MDIBC is shown in Figure 15 and 16 respectively, the input voltage supplied here is 200 Volts, as amount of parallel switches per phase increases the ripple content is reduced and frequency of output is increased which is easy to filter out.

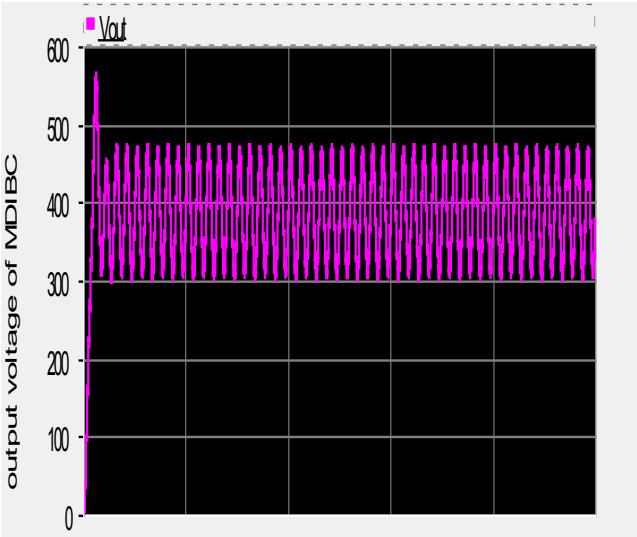

Figure 13. Output voltage Waveform of MDIBC (2-pole, 2-phase).

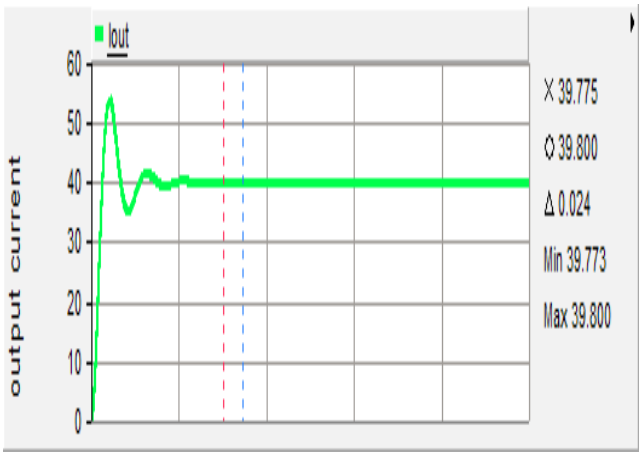

Figure 14. Output current Waveform of MDIBC (2-pole, 2-phase).

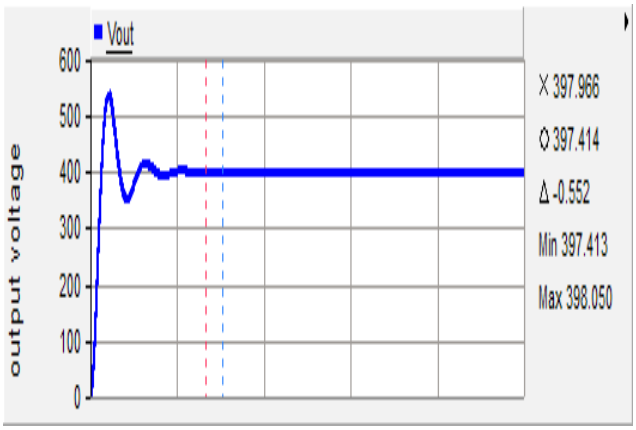

Figure 15. output voltage waveform of Four-pole three-phase MDIBC.

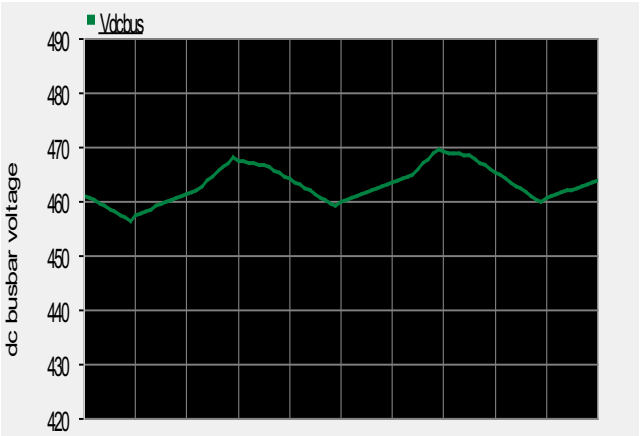

Figure 16. output current waveform of Four-pole three-phase MDIBC.

6. Conclusion

The output of the MDIBC has less ripple content when compare that of Boost and Multidevice boost converter, as the number no phases and no of parallel switches per phase increases the requirement of filter size is reduced due reduction in the ripple content, the reduction in the advances the system performance which as the size of filter components reduces the overall weight of the system reduces which is an important parameter for the Aircraft systems which as Photovoltaic cells has only power source and overall system has low. Using bidirectional dc-dc converter to transfer power between the battery and PV cell and between PV cell and electric sink makes the entire system to be highly reliable and renders to supply power to motor and other electric load during night flights.

7. References

1. Ahmad A, Paulson S and Amar Y. Ministry New Renew. Energy, Government India: Solarizing India: Tapping the excellent potential renewable energy. 2016; 9(3):13–7.
2. Mallikarjuna Reddy B, Narendra CH, Rambabu CH. A ZVS PWM Three-Phase current fed push-pull DC-DC converter with fuel cell input. IJSETR. 2014; 3(12):3449–54.
3. Swati D, Jayaram Kumar SV. Analysis of wind driven self-excited induction generator connected to grid interface with multi-level inverter. IJST. 2011; 1(3):19–25.
4. Yoshida S, Ueno S, Kataoka N, Takakura H and Minemoto T. Estimation of global tilted irradiance and output energy using meteorological data and performance of photovoltaic modules. Solar Energy. 2013; 93:90–9.
5. Ahmad A, Akhilesh KG and Paulson S. HDL Co-Simulation of Single Phase Z-Source Inverter. Allahabad, India: 2nd IEEE Students, Conference on Engineering and Systems of 3rd SCES: MNNIT. 2013.
6. Gautham R and Sundereson P and Umanand L. A New bi-directional topologies for electrical drives. Journal of Indian institute of Science. 2000; 80:319–26.
7. Karthik DR, Mallikarjuna Reddy B, Reddy Praveen Kumar. A ZVS PWM Three-Phase current fed push-pull DC-DC converter in Microgrids. IJSETR. 2015; 4(8):2783–92.
8. Ahmad A, Paulson S. Mixed Simulation of Electrical power converters using MATLAB and Modelsim. India: E-mantha: IEEE Conference. 2012; p. 700–3.
9. Bharathi ML, Kirubakaran D. Comparative Study on Solar Powered Interleaved Boost Converter. Indian Journal of Science and Technology. 2015; 8(3):123–9.
10. Karthik DR, Mallikarjuna Reddy B, Singh Satendra Kumar. A PSCAD simulation on integration of multi-level inverters with the DC_DC converters for the AC motor applications. Tamilnadu: Noorul Islam University: ICCPCT conference. 2016. [In Press].
11. Saravanan, Srinivasan V, Sandiya VP. A Two Stage DC-DC Converter with Isolation for Renewable Energy Applications. Indian Journal of Science and Technology. 2013; 6(6):321–7.
12. Mallikarjuna Reddy B, Samuel Paulson. A comparative analysis of non-isolated bi-directional dc-dc converters. IEEE power electronics society conference, July-2016. [In Press].